



16th International Scientific Conference “Chemistry and Chemical Engineering in XXI century”
dedicated to Professor L.P. Kulyov, CCE 2015

Adsorption of Ar and N₂ on dealuminated mordenite tuffs

Karla Ortega^a, Miguel Angel Hernandez^{b,*}, Roberto Portillo^c, Edgar Ayala^a, Omar Romero^b, Fernando Rojas^d, Efrain Rubio^e, Alexey Pestryakov^f, Vitalii Petranovskii^g

^aFacultad de Ingeniería Química, BUAP, Puebla, Mexico

^bDepartamento de Investigación en Zeolitas y Posgrado en Agroecología, Instituto de Ciencias, BUAP, Puebla, Mexico

^cFacultad de Ciencias Químicas, BUAP, Puebla, México

^dDepartamento de Química, Universidad Autónoma Metropolitana-Iztapalapa, Apartado Postal 55-534, México 09340, D.F.

^eCentro Universitario de Vinculación y Transferencia de Tecnología, BUAP, Puebla, Mexico

^fTomsk Polytechnic University, Tomsk 634050, Russia

^gCentro de Nanociencias y Nanotecnología, Universidad Nacional Autónoma de México, Carretera Tijuana-Ensenada, Km. 107, Ensenada, B.C. Mexico; On the sabbatical leave at: Departamento de Investigación en Zeolitas, Instituto de Ciencias BUAP, Puebla 72570, México

Abstract

This paper describes the adsorption of nitrogen and argon on pores in natural mordenites before and after acid leaching treatment. The exchange with H⁺ ions during dealumination favors the creation of emergent pores thus causing an increase of the adsorption capacity. The development of nanopores in mordenites was evaluated through the Dubinin-Astakhov and Barrett-Joyner-Halenda methods.

© 2015 The Authors. Published by Elsevier B.V. This is an open access article under the CC BY-NC-ND license (<http://creativecommons.org/licenses/by-nc-nd/4.0/>).

Peer-review under responsibility of Tomsk Polytechnic University

Keywords: mordenite ; tuff ; argon ; nitrogen ; adsorption ; dealumination

1. Introduction

There are more than 200 zeolite types with different structure of channels and cavities¹. Nevertheless, despite the continued increase in the availability of new molecular sieve materials and the associated research activities into

* Corresponding author. Tel.: +52(222) 229-5500, ext. 7270

E-mail address: vaga1957@gmail.com

their applications, only a handful are used in more than one industrial process (MFI, BEA, MOR, FER, FAU, LTL, CHA)². A zeolite that is commonly used in many applications is mordenite (MOR according to IZA codes³). Mordenite is widespread in nature; it may be obtained synthetically as well. It is one of the most common natural zeolites and is extensively used commercially. In Mexico, mordenite deposits are known in Cruillas Tamaulipas Chalma, State of Mexico, La Magdalena, Oaxaca, El Viejo/Apo, Tumbiscatio, Michoacán, etc.^{4,5}

The chemical composition of a prototype mordenite is $\text{[Na}_8(\text{H}_2\text{O})_{24}\text{] [Al}_8\text{Si}_{40}\text{O}_{96}]^6$. The Si/Al atomic ratio is equal to 5 for pure mordenite phase; but it can be varied in some limits. Dealumination by acid treatment lead to the significant changing of mordenite composition, and moieties with Si/Al ratios up to 100 can be obtained. In the same time, formation of a secondary porosity (i.e., mesopores) is observed⁷.

Porosity in mordenite is presented by two types of channels. The first one is formed by the assemblage of 12-membered rings, each of which having 12 oxygen atoms. The second one is formed by 8-membered rings (in which there are 8 oxygen atoms). The porous structure of mordenite consists of a channel system in which 12-membered ring channels run parallel to the [001], or *c* axis, and 8-membered ones are parallel to [010], or *b* axis^{1,7}. Free diameters of the 12-membered elliptic channels are 0.65-0.70 nm, while free diameters of the 8-membered elliptic windows are 0.26-0.57 nm. Channels 1 and 2 are interconnected in the form of small side pockets along the [010] axis^{1,8}. Maximum diameter of a sphere that can diffuse along *b* channel is equal to 2.95 Å, and the same for *c* channel is 6.45 Å^{1,3}. Thus, the channel system is essentially a 2-dimensional network with elliptical 12-ring apertures. Diffusion is limited in the [010], or *b* direction.

Cation sites reside in the centers of the 8-membered rings that are parallel to either *c* or *b*. These sites are regularly occupied, thus leading to pore blocking and leaving the 12-membered channels as the only ones for molecular diffusion. It was observed that mordenite allows the passage of molecules not greater than 0.42 nm. Natural mordenites, enriched with alkali cations, can be unblocked after treatment with dilute hydrochloric acid⁹. This paper presents an experimental study on the adsorption of Ar and N₂ in natural mordenites, both for the freshly obtained and treated with HCl at different concentrations samples.

2. Experimental Section

For this work were selected natural Mexican mordenites from La Magdalena, Oaxaca, and Cruillas, Tamaulipas, labeled as MOR6 and MOR9 respectively. These labels accounts for the natural samples, those are free of any chemical treatment. A zeolitic rock was milled, and fraction with mesh 60-80 (diameter in the range of +150-250 μm) was selected for the experimental work. As a reference sample was used synthetic mordenite supplied by Zeolyst Int., labeled as MORS.

Samples of dealuminated mordenite were prepared by an acid-leaching process of the precursors; this leaching process caused the exchange of polyvalent cations by protons, and the removal of framework aluminum and mineral impurities¹⁰. This modification procedure consisted of a series of washing cycles of natural mordenite samples with dilute HCl, followed by prolonged rinses with deionized water. Each of the steps of the HCl washing procedure was made at 50 °C during 6 h with 1.0 N HCl. After washings a sample of natural zeolite MOR9 in HCl solution once, twice or three times, the samples were labeled as H1, H2 and H3.

N₂ and He ultrahigh purity gases (> 99.999%, INFRA Corp.) were employed for the textural sorption studies of natural, synthetic and dealuminated mordenites. All N₂ adsorption isotherms were measured at the boiling point of liquid N₂ (76.4 K at the 2200 m altitude of Puebla City, México) in an automatic volumetric adsorption system (Quantachrome AutoSorb-1LC). Prior to the sorption experiments, samples were outgassed at 623 K during 20 h at a pressure lesser than 10⁻⁶ mbar. XRD patterns were determined by means of a Siemens D-500 diffractometer employing a nickel filtered Cu K_α radiation and compared with the corresponding JCCPD files. Scanning Electron Microscopy images were obtained from a Vega Tescan, model JSM-5300 electron microscope equipped with an energy dispersive spectrometer (EDS) probe.

3. Results and discussion

The channel system of mordenite is essentially a 2-dimensional network with elliptical 12-ring apertures. Diffusion is limited in the [010], or *b* direction. The mordenite channel structure can be seen in Figure 1.

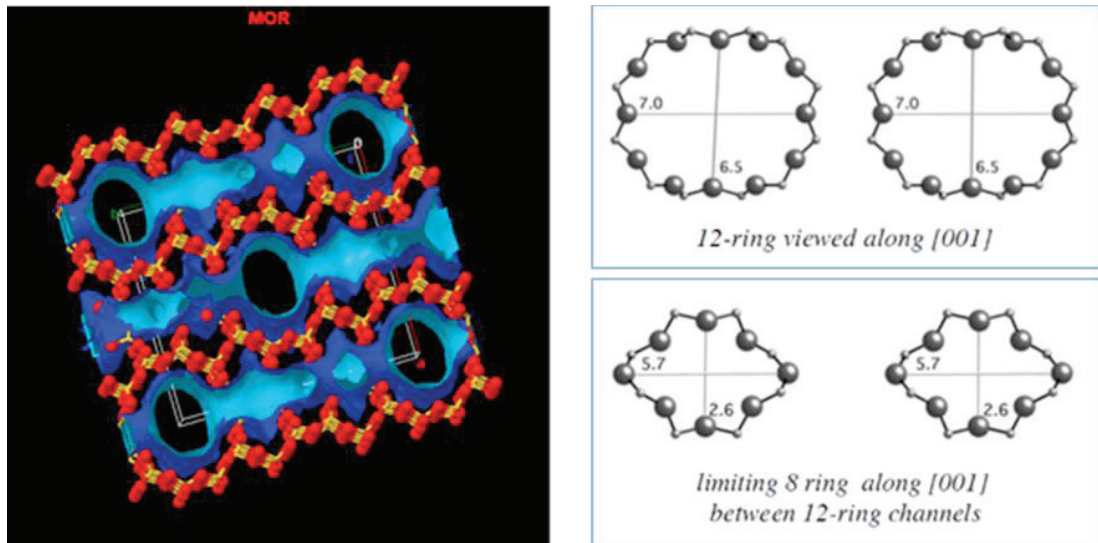


Fig. 1. Structure of mordenite. Left side - three-dimensional simulation that schematically shows Si and O ions (yellow and red bolls, respectively) and internal surface of channels, light-blue surface. The parallelepiped frame represents elementary cell. Right side – rings in the openings of mordenite channels.

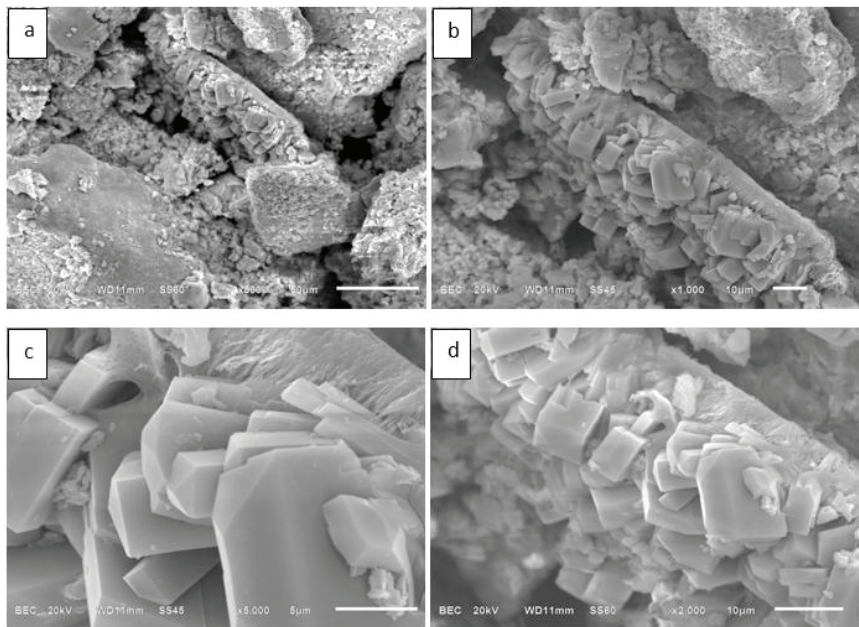


Fig. 2. SEM images of natural mordenite with different amplifications: (a) x800; (b) x1000; (c) x5000; (d) x2000

X-ray diffraction patterns of mordenite samples (not shown) are typical for these materials⁸. Variation in sharpness of the observed peaks reflects variation of crystallinity of these substrates. Conclusion was made that MOR6 has the lowest crystallinity, in contrast to a high crystallinity observed for the synthetic MORS and natural MOR9 mordenites. The presence of small amounts of quartz (JCPDS 3-0427) and kaolinite (JCPDS 001-0527) in the sample MOR6 was observed¹¹.

SEM images (Figure 2) show the presence of aggregates of thin plate-shaped crystals with varying geometry. Sizes of observed crystals are less than 10 μm . EDS analysis demonstrates that both natural zeolites (MOR6 and MOR9) are low-silica mordenites. Experimental Si/Al value for MOR6 is lower than five, the lowest possible limit for mordenites⁶; presumably, the quartz and kaolinite impurities are responsible for observed difference. For both MOR6 and MOR9 samples considerable amounts of Na are detected, see Table 1.

Table 1. Mordenite chemical composition (mass %) measured by EDS.

Sample	SiO ₂	Al ₂ O ₃	Fe ₂ O ₃	CaO	MgO	Na ₂ O	K ₂ O	Si/Al	PxC
MOR6	74.2	17.6	-	1.0	0.8	5.2	-	4.2	1.9
MOR9	72.1	12.0	0.83	2.0	-	6.0	1.2	5.3	5.9

Argon sorption on natural MOR9 mordenite is similar to N₂ sorption. The isotherm displays an open and slightly wider hysteresis loop compared to the case of N₂. However adsorption is not as sharp at low relative pressures as it is in the case of N₂, it happens that cation interactions with Ar are weaker than with N₂. Again, there is evidence of the existence of lamellar impurities in the sample. The results of the textural studies are reported in Table 2. This Table shows the establishment of the following sequence for the estimated by the BET method values of specific surface A_{SB}: MORS > MOR9 > MOR6. For total pore volume V_Σ sequence is: MOR9 > MORS > MOR6.

Table 2. Textural parameters of natural and synthetic mordenites^a.

Sample	A _{SL} m ² g ⁻¹	A _{SB} m ² g ⁻¹	V _Σ cm ³ g ⁻¹	C _B	PD _{DA} nm	W _{0ms}	V _{meso} cm ³ g ⁻¹	Purity %
MORS	425.0	301.0	0.153	-0.56	0.65	0.152	0.0009	99.35
MOR6	154.5	111.4	0.128	-0.16	0.66	0.035	0.0929	27.34
MOR9	404.6	281.8	0.186	-0.16	0.67	0.122	0.0645	65.59
MOR9Ar	112.3	78.3	0.053	-180	0.76	0.023	0.030	43.39

^aA_{SL}, Langmuir specific surface area; A_{SB}, BET specific surface area; C_B, BET constant; V_Σ, volume adsorbed at $p/p^0 = 0.95$ and expressed as the volume of liquid N₂ (Gursvitch rule); W₀, volume micropore estimated from t -plots; V_{meso} = V_Σ - W₀ and purity.

N₂ adsorption-desorption isotherms on natural MOR9 and synthetic MORS mordenite specimens are shown in Figure 3. The shape of MOR9 isotherm is a combination of Types I and IV isotherms; the hysteresis loop is open and includes both low- and high-pressure narrow hysteresis loops¹². The shape H3 of the hysteresis cycle at high pressure suggests that a small amount of non-crystalline materials of lamellar type (natural kaolinite, observed by DRX) exist in between the crystallites. The isotherm of synthetic sample MORS corresponds to a Type I and shows a very steep sorption uptake at low pressures. This saturation region (in the sense that all micropores are already filled) extends between $0.1 < p/p^0 < 0.9$. At higher relative pressures, there is still no substantial increase of the sorption capacity, thus indicating that the sample is very pure indeed, since no mesopores are present as neither multilayer adsorption nor capillary condensation develops therein. However, low-pressure hysteresis can also be observed in the synthetic sample as with the natural samples. Figure 3b portrays the evolution of the shapes of the N₂ isotherms with respect to the number of HCl washings. The MOR9, H1 and H2 substrates render type IV isotherms (with extremely narrow hysteresis loops). Distinctive features of these types of isotherms are as follows:

- (i) the extent of microporosity in dealuminated mordenite decreases, in general, with the number of acid treatments; the plateaus of the N₂ isotherms corresponding to H mordenites reach decreasing heights according to the accessible microporosity depicted by each zeolite; and
- (ii) the existence of a low-pressure hysteresis region is evident for all specimen.

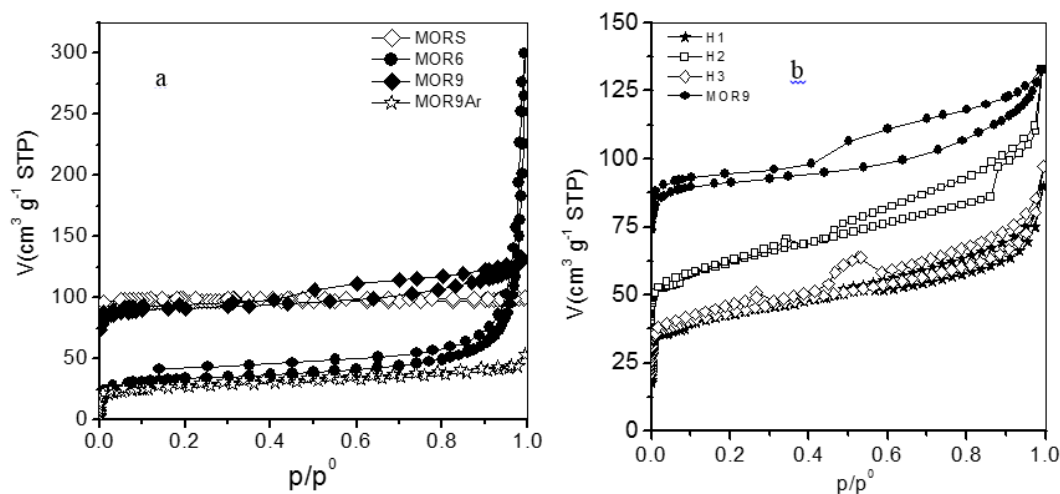


Fig. 3. N₂ adsorption isotherms on MORS, MOR6 and MOR9 (part a, left) and the same isotherms on MOR6, H1 and H2 (part b, right).

It is also important to note that dealuminated mordenites possess a microporous volume several times minor than that of MOR9. Therefore, acid treatment of high-silica natural mordenites can render adsorbents of inaccessible pore volumes via the mechanism of decationation and dealumination and also clean it by dissolution of amorphous materials blocking the entrances to the channels of the mordenite structure. The cation blocking effects at pore entrances in natural mordenite are thus diminished by acid treatment, then lowering the cation-exchange capacity of the resultant substrates by leaching out Al³⁺ from framework positions and introducing H⁺ into the remaining cation sites of the natural precursor.

Important textural parameters of mordenites are listed in Table 3. For the H Mordenites, the BET equation CB constants are sometimes negative, and this can be explained by the fact that multilayer adsorption in micropores is not a plausible model therein.

Table 3. Textural parameters of modified natural MOR9 mordenite^a, determined from N₂ adsorption.

Sample	A _{SL} m ² g ⁻¹	A _{SB} m ² g ⁻¹	V _Σ cm ³ g ⁻¹	C _B	PD _{DA} nm	W _{0.05}
MOR9	404.6	281.6	0.186	-120	0.67	0.122
H1	158.7	109.2	0.111	-62	0.765	0.040
H2	205.8	139.6	0.111	-99	0.763	0.053
H3	210.9	142.78	0.120	-105	0.765	0.067

^aA_{SL}, Langmuir specific surface area; A_{SB}, BET specific surface area; C_B, BET constant; V_Σ, volume adsorbed at p/p⁰ = 0.95 and expressed as the volume of liquid N₂ (Gursvitch rule).

Filling of the wider channels of the mordenite structure was evaluated through Dubinin-Astakhov (D-A) method⁹ of nanopore size distribution determination, assuming a cylindrical shape of the nanochannels of this zeolite, Fig. 4a. According to this equation, the process of larger channels filling is the main contribution to the adsorbed volume. The results indicate the uniformity of these channels centered between 0.765 and 0.781 nm values, see the sixth column of Table 3.

Fig. 4b shows the distribution curves obtained using the Barrett-Joyner-Halenda mesopores equation. The H2 sample shows a trimodal distribution with pore diameters located at 2.0, 3.6 and 4.5 nm, whereas natural zeolites and H1 and H2 exhibit a bimodal character, with values in 1.8 and 3.8 nm.

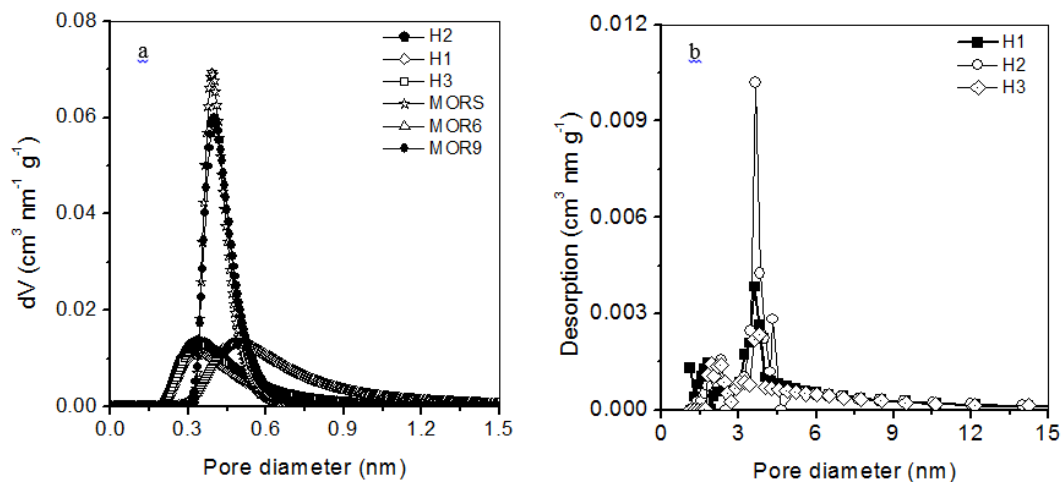


Fig. 4. Nanoporosity size distribution on MORS, MOR6 and MOR9 (part a, left), calculated with DA equation, and pore size distribution for the isotherms samples (part b, right), calculated with BJH equation.

4. Conclusions

The natural mordenite zeolites were evaluated by various adsorption characterization techniques. Dealuminated and decationated mordenites H2 and H3 are less favorable in terms of their porosity. The measured adsorption characteristics allow us to suggest the following conclusions regarding the porous structures of our mordenite adsorbents: (i) MOR9 pore entrances are inaccessible for Ar and N₂ molecules; this is likely due to the presence of bulky ionic species at these entrance points; (ii) MOR9 is an open microporous structure in which primary and secondary micropore filling mechanisms take place. The existence of a low-pressure hysteresis loop associated with this substrate can mean that microporous channels are either interconnected to each other by thin capillaries, or surrounded by narrow cracks that appear due to the dealumination process.

Acknowledgements

This work was supported by the VIEP and CUVyTT, the Academic Body "Investigación en zeolitas", CA-95 (PROMEP-SEP). The authors acknowledge funding for this research by the Russian Government Program «Science» of Tomsk Polytechnic University, grant No. 4.1187.2014/K, and by UNAM-PAPIIT, Mexico, through the grant IN110713. V. Petranovskii thankful to DGAPA-UNAM for support of his sabbatical stay in BUAP.

References

1. Baerlocher Ch, McCusker LB, Olson DH. *Atlas of zeolite framework types*. 6th ed. Amsterdam: Elsevier; 2007.
2. Perego C, Carati A. Zeolites and zeolite-like materials in industrial catalysis. In: Cejka J, Perez-Pariente J, Roth WJ, editors. *Zeolites: from model materials to industrial catalysts, Chapter: 14*. Kerala, India: Transworld Research Network; 2008. 37/661, p. 357-389.
3. <http://www.iza-structure.org/databases/>
4. Wise WS. *Handbook of Natural Zeolites*, Naples: De Frede Editore; 2013.
5. Hernández MÁ, Rojas F, Corona L, Lara VH, Portillo R, Salgado MA, Petranovskii V. Evaluación de la Porosidad de Zeolitas Naturales por Medio de Curvas Diferenciales de Adsorción. *Rev Int Contaminación Ambiental* 2005;21:71-81.
6. Breck DW. *Zeolite Molecular Sieves*. New York: Wiley-Interscience; 1974.
7. Silaghi MC, Chizallet C, Raybaud P. Challenges on molecular aspects of dealumination and desilication of zeolites. *Micropor Mesopor Mater* 2014;191:82-96.
8. Treacy MMJ, Higgins JB. *Collection of Simulated XRD Powder Patterns for Zeolites*, 5th ed. Amsterdam: Elsevier; 2007.

9. Hernández MA, Rojas F, Portillo R, Salgado MA, Corona L. Nanoporosity on natural and dealuminated zeolites from Mexico, Proc. *Zeolite 2014 – 9th International Conference on the Occurrence, Properties and Utilization of Natural Zeolites*. Daković A, Trgo M, Langella A, editors. Serbia: INZA, 2014; 95-96.
10. Hernández MA, Rojas F, Lara VH, Portillo R, Castelán R, Pérez G, Salas R. Estructura porosa y propiedades estructurales de Mordenita y clinoptilolita. *Superficies y Vacío* 2014;**23**:51-56.
11. Hernández MA, Rojas F, Portillo R, Petranovskii V, Salgado MA. Influence of the Si/Al Framework Ratio on the Microporosity of Dealuminated Mordenite as Determined from N₂ Adsorption. *Separation Science and Technology* 2006;**41**:1907-25.
12. Sing KSW. Characterization of porous materials: past, present and future. *Coll Surf* 2004;**241**:3-7.